Preprints of the 21st IFAC World Congress (Virtual)
Berlin, Germany, July 12-17, 2020

A Novel Strategy for High-Performance Vehicle Lateral Motion Control

X. Yin* A. Eckert*

** Research & Advanced Engineering*
Holistic Engineering and Technologies
Continental Teves AG & Co. oHG, Frankfurt am Main, Germany
(e-mail: xiuxun.yin@ continental.com,
alfred.eckert@ continental.com)

Abstract: This paper presents a new design strategy for vehicle lateral motion control. In particular, the controller design problem for vehicle path following is considered. A new kind of full error-state dynamic equation incorporating more significant error states is introduced, which describes vehicle lateral dynamics with respect to the desired path, even without the curvature of the desired path acting as disturbance at the input. Thus, the feedback and the feedforward controller can be designed straightforwardly. A novel solution is provided to extract the desired feedforward steering command and the desired reference states from the varying curvature of the desired path. Simulation results demonstrate the efficiency, high performance and robustness of the developed control strategy.

Keywords: Automotive Control, Intelligent Autonomous Vehicles, Control Design, Path Following and Trajectory Tracking, Vehicle Motion Control, Tracking Control.

1. INTRODUCTION

Lateral vehicle motion control is an essential part for automated driving such as Highway Cruising Chauffeur, Lane Keeping Assist, Lane Change Assist and Emergency Steering Assist. For decades, researchers have been engaged in developing lateral controllers and many control schemes have been investigated. Nowadays, car makers and suppliers are developing lateral controllers for driver assistance, highly and fully automated driving systems under more realistic conditions considering sensor noise, actuator dynamics, road conditions, robustness, safety constraints and the complexity of the algorithm to embed the control algorithm into cost efficient ECUs (Electro Control Unit).

Many model-based design methods have been approached for vehicle lateral motion control (Kapania et al. 2015, Ni et al. 2016, Tange et al. 2016, Schmeitz et al. 2017). Most of the model-based design methods for vehicle lateral control deploy a so-called vehicle lateral error-state dynamic equation based on the well-known linear bicycle model. There are mainly two slightly different forms of error-state equations: one (Kramer 2008) uses the vehicle side-slip angle as one of the state variables while the other (Rajamani 2012) uses the vehicle lateral speed as a state variable. Both error-state equations define the yaw angle error and the lateral position error of the vehicle with respect to the desired path as error states. The main drawbacks of these error-state equations are: firstly, they exclude other potentially useful states such as yaw rate, side-slip angle and steering angle as error states. However, including these as error states can greatly improve the lateral tracking performance. Secondly, the varying curvature of the path acts as a disturbance input in both error-state equations, which makes the design of the lateral motion controller nontrivial. Some case dependent solutions to compensate for the known curvature as disturbance input are given by Rajamani (2012), Marino et al. (2009). Yin (2010) discusses a similar solution for the same cases while considering vehicle EPS (Electric Power Steering) dynamics. However, general solution for this problem does not seem to be available yet.

In this paper, we present a new control strategy that removes the weaknesses of the known methods and enhances the control performance. The proposed control strategy provides a novel approach using a new kind of full error-state vehicle lateral dynamic equation. Furthermore, it introduces a desired states observer, which extracts the desired reference states and the desired feedforward steering control command from the curvature of the path to be followed.

The paper is structured as follows. In Section 2, we introduce the vehicle lateral dynamics and formulate the objective of the lateral motion control. Section 3 presents a new full error-state dynamic equation, which eliminates the road curvature as disturbance at the model input. In Section 4, the desired feedforward steering command and the reference states observer is derived. Section 5 demonstrates the efficiency, the performance and the robustness of the control strategy through numerical simulation. Finally, conclusions are drawn in Section 6.

2. PROBLEM FORMULATION

2.1 Vehicle lateral dynamics

The linear bicycle model, as schematically shown in Figure 1, describes vehicle lateral dynamics for a given constant longitudinal velocity v_x (Mitschke et al. 2004)

$$\dot{\beta} = \frac{-(c_r + c_f)}{m v_x}\beta + \left(\frac{c_r l_r - c_f l_f}{m v_x^2} - 1\right)\dot{\psi} + \frac{c_f}{m v_x}\delta \ , \quad (1)$$

$$\ddot{\psi} = \frac{c_r l_r - c_f l_f}{J_z}\beta + \frac{-(c_r l_r^2 + c_f l_f^2)}{J_z v_x}\dot{\psi} + \frac{c_f l_f}{J_z}\delta \ , \quad (2)$$

where m and J_z are the vehicle mass and inertia. c_f and c_r are the front and rear tire cornering stiffness and l_f and l_r are the distance of the front and rear wheel axle from the vehicle centre of gravity, respectively. β and $\dot{\psi}$ are the side slip angle and the yaw rate, while δ is the steering angle of the front wheel.

The steering angle δ is set by a low-level steering angle controller through the EPS actuator. The dynamics of the steering angle controller and the EPS actuator can be modelled as:

$$\dot{\delta} = a_{11}\delta + b\delta_c \ , \quad (3)$$

with δ_c the steering angle command as input. a_{11} and b are model parameters which are identified from the experimental measurements.

Defining a_{21} to a_{33} as:

$$a_{21} = \frac{c_f}{m v_x} \ , a_{22} = \frac{-(c_r + c_f)}{m v_x} \ , \ a_{23} = \frac{c_r l_r - c_f l_f}{m v_x^2} - 1,$$

$$a_{31} = \frac{c_f l_f}{J_z} \ , a_{32} = \frac{c_r l_r - c_f l_f}{J_z} \ , \ a_{33} = \frac{-(c_r l_r^2 + c_f l_f^2)}{J_z v_x},$$

equation (1) and (2) can be rewritten as:

$$\dot{\beta} = a_{22}\beta + a_{23}\dot{\psi} + a_{21}\delta \ , \quad (4)$$

$$\ddot{\psi} = a_{32}\beta + a_{33}\dot{\psi} + a_{31}\delta \ . \quad (5)$$

The equations (3) to (5) can be written in state space form

$$\begin{bmatrix}\dot{\delta}\\ \dot{\beta}\\ \ddot{\psi}\end{bmatrix} = \begin{bmatrix}a_{11} & 0 & 0\\ a_{21} & a_{22} & a_{23}\\ a_{31} & a_{32} & a_{33}\end{bmatrix}\begin{bmatrix}\delta\\ \beta\\ \dot{\psi}\end{bmatrix} + \begin{bmatrix}b\\ 0\\ 0\end{bmatrix}\delta_c \ . \quad (6)$$

The lateral dynamics at the vehicle's CoG (centre of gravity), with respect to a desired path, can be described (Li et al. 2005) as:

$$\dot{\psi}_{\mathrm{L}} = \dot{\psi} - v\kappa_r \ , \quad (7)$$

$$\dot{y}_L = v\beta + v\psi_L \ , \quad (8)$$

where v is the vehicle speed at the vehicle centre of gravity, y_L is the lateral deviation of the vehicle's CoG to the desired path, ψ_L is the yaw angle error of the vehicle relative to the path and κ_r is the path curvature as depicted in Figure 1.

The model (6) to (8) can be compactly written as:

$$\begin{bmatrix}\dot{\delta}\\ \dot{\beta}\\ \ddot{\psi}\\ \dot{\psi}_{\mathrm{L}}\\ \dot{y}_L\end{bmatrix} = \begin{bmatrix}a_{11} & 0 & 0 & 0 & 0\\ a_{21} & a_{22} & a_{23} & 0 & 0\\ a_{31} & a_{32} & a_{33} & 0 & 0\\ 0 & 0 & 1 & 0 & 0\\ 0 & v & 0 & v & 0\end{bmatrix}\begin{bmatrix}\delta\\ \beta\\ \dot{\psi}\\ \psi_L\\ y_L\end{bmatrix} + \begin{bmatrix}b & 0\\ 0 & 0\\ 0 & 0\\ 0 & -v\\ 0 & 0\end{bmatrix}\begin{bmatrix}\delta_c\\ \kappa_r\end{bmatrix}. \quad (9)$$

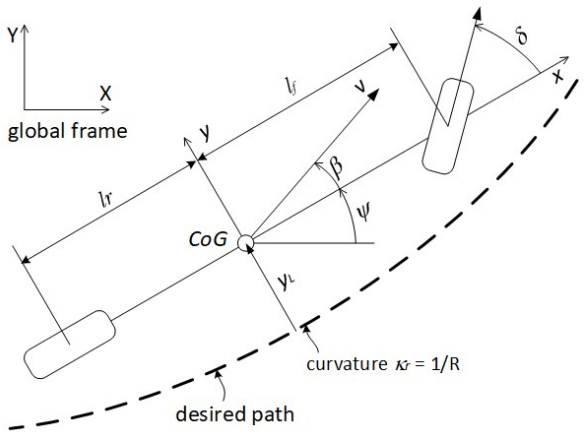

Fig. 1. Vehicle bicycle model and desired path in the global frame.

For a constant velocity, this model describes an LTI-system with the control input δ_c and the disturbance input κ_r.

In a real vehicle system, the steering angle δ, the yaw rate $\dot{\psi}$ and the longitudinal velocity v_x can be measured through ESC (Electronic Stability Control)-sensors and the side slip angle β can be estimated through a model-based observer.

The yaw angle error ψ_L, the lateral deviation y_L of the vehicle with respect to the desired path and the path curvature κ_r can be detected by the camera for the path following control.

Our focus in this paper is to develop a lateral motion controller, therefore, we assume that the state variables in (9) can be measured.

2.2 Control objective

The objective of vehicle lateral motion control for the given system (9) with feasible desired path κ_r is to find a feedback control input δ_c as a function of the available states in (9) and the curvature κ_r of desired path such that

$$\delta_c = u(\delta, \beta, \dot{\psi}, \psi_L, y_L, \kappa_r) \quad (10)$$

and that the closed loop control system

$$\begin{bmatrix}\dot{\delta}\\ \dot{\beta}\\ \ddot{\psi}\\ \dot{\psi}_{\mathrm{L}}\\ \dot{y}_L\end{bmatrix} = \begin{bmatrix}a_{11} & 0 & 0 & 0 & 0\\ a_{21} & a_{22} & a_{23} & 0 & 0\\ a_{31} & a_{32} & a_{33} & 0 & 0\\ 0 & 0 & 1 & 0 & 0\\ 0 & v & 0 & v & 0\end{bmatrix}\begin{bmatrix}\delta\\ \beta\\ \dot{\psi}\\ \psi_L\\ y_L\end{bmatrix}$$

$$+\begin{bmatrix} b & 0 \\ 0 & 0 \\ 0 & 0 \\ 0 & -v \\ 0 & 0 \end{bmatrix}\begin{bmatrix} u(\delta,\beta,\dot{\psi},\psi_L,y_L,\kappa_r,v) \\ \kappa_r \end{bmatrix} \quad (11)$$

guarantees the rapid convergence of the lateral deviation y_L of the vehicle to zero with a bounded lateral acceleration.

3. CONTROL STRATEGY

The vehicle lateral motion control formulated in (9) falls under the tracking control problem. If we can find the reference states for (9), then the lateral position tracking can be formulated as an error-states regulation problem and all regulator design methods can be applied.

In the following, we derive an error-state equation from (9). In particular, we convert the feasible curvature κ_r of the desired path into an equivalent steering command with the corresponding reference states, thus eliminating the curvature disturbance at the input.

Normally, the curvature of a road is designed in such a manner that a vehicle can track the lane for the prescribed speed. In case of trajectory tracking, the trajectory planner guarantees that the planned trajectory can be tracked by the vehicle. This means that there always exists a steering command, which ensures that the vehicle can follow the desired path accurately.

For the construction of such a steering command from the path curvature and the vehicle dynamics (6), we assume a virtual vehicle that moves with the real vehicle on the path as depicted in Figure 2. The virtual vehicle's CoG coincides with the desired path at the minimal distance between desired path and the CoG of the real vehicle at any given time.

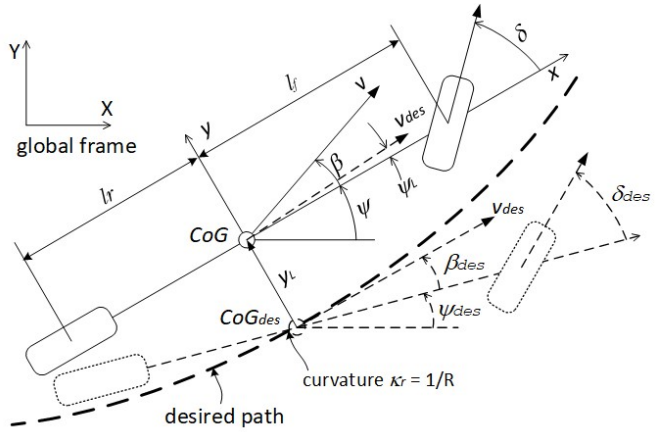

Fig. 2. Virtual vehicle with the accurate tracking of the desired path.

We assume that the lateral dynamics of the virtual vehicle is the same as for the real vehicle, so that its lateral dynamics comply with (6). We refer to this virtual vehicle hereinafter as the desired vehicle and denote its states and input with subscript "*des*" for "desired". Then the desired vehicle dynamics can be described as:

$$\begin{bmatrix} \dot{\delta}_{des} \\ \dot{\beta}_{des} \\ \ddot{\psi}_{des} \end{bmatrix} = \begin{bmatrix} a_{11} & 0 & 0 \\ a_{21} & a_{22} & a_{23} \\ a_{31} & a_{32} & a_{33} \end{bmatrix}\begin{bmatrix} \delta_{des} \\ \beta_{des} \\ \dot{\psi}_{des} \end{bmatrix} + \begin{bmatrix} b \\ 0 \\ 0 \end{bmatrix}\delta_{cdes}\,. \quad (12)$$

Both (6) and (12) are linear systems and obey the superposition principle. Therefore, with the notation

$$\begin{bmatrix} \delta_e \\ \beta_e \\ \dot{\psi}_e \end{bmatrix} = \begin{bmatrix} \delta \\ \beta \\ \dot{\psi} \end{bmatrix} - \begin{bmatrix} \delta_{des} \\ \beta_{des} \\ \dot{\psi}_{des} \end{bmatrix}, \quad (13)$$

we derive from (6) and (12) the following error dynamics of the real and the desired vehicles

$$\begin{bmatrix} \dot{\delta}_e \\ \dot{\beta}_e \\ \ddot{\psi}_e \end{bmatrix} = \begin{bmatrix} a_{11} & 0 & 0 \\ a_{21} & a_{22} & a_{23} \\ a_{31} & a_{32} & a_{33} \end{bmatrix}\begin{bmatrix} \delta_e \\ \beta_e \\ \dot{\psi}_e \end{bmatrix} + \begin{bmatrix} b \\ 0 \\ 0 \end{bmatrix}(\delta_c - \delta_{cdes}). \quad (14)$$

The track angle of the desired vehicle is defined as the velocity angle of the vehicle in the global frame shown in Figure 2. This is same as the yaw angle of the lane centreline, therefor,

$$\dot{\psi}_{des} + \dot{\beta}_{des} = v\kappa_r\,, \quad (15)$$

and equation (7) can be rewritten as:

$$\begin{aligned} \dot{\psi}_L &= \dot{\psi} - \dot{\psi}_{des} - \dot{\beta}_{des} \\ &= \dot{\psi}_e - \dot{\beta}_{des}\,, \end{aligned}$$

and equivalently

$$\psi_L = \psi_e - \beta_{des}\,. \quad (16)$$

As a result of (16), (8) can be formulated as a function of the error states β_e and ψ_e :

$$\begin{aligned} \dot{y}_L &= v\beta + v(\psi_e - \beta_{des}) \\ &= v\beta_e + v\psi_e \\ &= v_x\sqrt{1+\left(\frac{v_y}{v_x}\right)^2}\,(\beta_e + \psi_e) \\ &\approx v_x\,(\beta_e + \psi_e)\,, \end{aligned} \quad (17)$$

whereby $\left(\frac{v_y}{v_x}\right)^2$ is much less than 1 and is disregarded in (17).

Extending (14) with the new states ψ_e and y_L yields

$$\begin{bmatrix} \dot{\delta}_e \\ \dot{\beta}_e \\ \ddot{\psi}_e \\ \dot{\psi}_e \\ \dot{y}_L \end{bmatrix} = \begin{bmatrix} a_{11} & 0 & 0 & 0 & 0 \\ a_{21} & a_{22} & a_{23} & 0 & 0 \\ a_{31} & a_{32} & a_{33} & 0 & 0 \\ 0 & 0 & 1 & 0 & 0 \\ 0 & v_x & 0 & v_x & 0 \end{bmatrix}\begin{bmatrix} \delta_e \\ \beta_e \\ \dot{\psi}_e \\ \psi_e \\ y_L \end{bmatrix} + \begin{bmatrix} b \\ 0 \\ 0 \\ 0 \\ 0 \end{bmatrix}(\delta_c - \delta_{cdes}).$$

or rewritten in a simpler form

$$\dot{\boldsymbol{x}}_e = A_e\boldsymbol{x}_e + B_e\,(\delta_c - \delta_{cdes}) \quad (18)$$

with

$$\boldsymbol{x}_e = \begin{bmatrix} \delta_e \\ \beta_e \\ \dot{\psi}_e \\ \psi_e \\ y_L \end{bmatrix}, A_e = \begin{bmatrix} a_{11} & 0 & 0 & 0 & 0 \\ a_{21} & a_{22} & a_{23} & 0 & 0 \\ a_{31} & a_{32} & a_{33} & 0 & 0 \\ 0 & 0 & 1 & 0 & 0 \\ 0 & v_x & 0 & v_x & 0 \end{bmatrix}, B_e = \begin{bmatrix} b \\ 0 \\ 0 \\ 0 \\ 0 \end{bmatrix}.$$

Equation (18) describes the error dynamics of the vehicle with respect to the desired vehicle states. The state variables are solely composed of error states. To distinguish from those error-state equations where the states are only partially composed of error states, we define (18) as a full error-state equation.

In contrast to conventional vehicle lateral error-state equations, this full error-state equation has the following new features:

- There is no path curvature as a disturbance at the input. All linear regulator design methods can be easily used without "tinkering" a feedforward compensator for the path curvature as disturbance.

- Besides the lateral position error and yaw angle error, it incorporates more significant state errors such as yaw rate error, side-slip angle error and steering angle error as error states. This may lead to an improved tracking control performance with a full error-states feedback: the controller already reacts for the state errors of the steering angle, yaw rate and side-slip angle, even when the yaw angle error and the lateral position deviation are still zero or negligible but are tending to increase.

It is straightforward to design a LQR state space feedback controller for (18). Denoting such a state feedback controller designed with the LQR-method for (18) as δ_{LQR}, yields

$$\delta_{LQR} = -\boldsymbol{k}_c \boldsymbol{x}_e \,, \tag{19}$$

where $\boldsymbol{k}_c$ is a 1×5 feedback control coefficient matrix. Hence, the final vehicle lateral motion control command δ_c is given by

$$\delta_c = \delta_{LQR} + \delta_{cdes} \,. \tag{20}$$

A linear state feedback (19) designed with the LQR-method can guarantee that the error state of (18) converges to zero or to a certain desired small value.

Note that the error state of the yaw angle ψ_e in (18) is not directly available from the camera in case of lane following control. However, with the known desired side slip angle β_{des} and the camera measurement ψ_L, it can be calculated from (16) as follows

$$\psi_e = \psi_L + \beta_{des} \,. \tag{21}$$

We derived the full error-state dynamics (18) based on the linear bicycle model with a given constant longitudinal velocity v_x. The velocity of the real vehicle can vary depending on the driving situation. Experimental driving tests have shown that the linear bicycle model can describe vehicle lateral dynamics for varying driving speeds if the longitudinal acceleration is smooth enough. Hence, we can design the controller for different vehicle speeds with the speed dependent weights in matrices Q and/or R to obtain the desired control performance. Using MATLAB as the design tool, a speed dependent $\boldsymbol{k}_c(v)$ can be calculated for certain discrete speed values v_k as:

$$\boldsymbol{k}_c(v_k) = lqr\big(A_e(v_k), B_e(v_k), Q(v_k), R(v_k)\big) \tag{22}$$

for later use in the simulations or real vehicles.

4. DESIRED INPUT AND STATES OBSERVER

We derived the vehicle lateral error-state dynamics (18) given that all the desired states and the steering command in (12) are available. Now we develop a method to estimate these desired states and corresponding steering commands from the curvature of the desired path by means of a Luenberger observer.

In (15), a link is established between the lateral dynamics of the desired vehicle and the curvature of the desired path. Substituting the rate of change of the side slip angle $\dot{\beta}_{des}$ in (15) with the left side of (4) results in

$$\begin{aligned} v\kappa_r &= \dot{\psi}_{des} + a_{21}\delta_{des} + a_{22}\beta_{des} + a_{23}\dot{\psi}_{des} \\ &= a_{21}\delta_{des} + a_{22}\beta_{des} + (1 + a_{23})\dot{\psi}_{des} \,, \end{aligned} \tag{23}$$

or

$$v\kappa_r = C[\delta_{des} \;\; \beta_{des} \;\; \dot{\psi}_{des}]^T \tag{24}$$

with

$$C = [a_{21} \quad a_{22} \quad (1 + a_{23})] \,. \tag{25}$$

Now we reconstruct (12) (Eyckhoff 1974) and use the Luenberger observer to estimate desired vehicle states and the desired steering command. For this purpose, we treat the steering command δ_{cdes} of the desired vehicle as a new state variable and rewrite (12) as

$$\begin{bmatrix} \dot{\delta}_{des} \\ \dot{\beta}_{des} \\ \ddot{\psi}_{des} \\ \dot{\delta}_{cdes} \end{bmatrix} = \begin{bmatrix} a_{11} & 0 & 0 & b \\ a_{21} & a_{22} & a_{23} & 0 \\ a_{31} & a_{32} & a_{33} & 0 \\ 0 & 0 & 0 & 0 \end{bmatrix} \begin{bmatrix} \delta_{des} \\ \beta_{des} \\ \dot{\psi}_{des} \\ \delta_{cdes} \end{bmatrix}. \tag{26}$$

It can be easily proven that the states of the system (26) with the measurement equation (24) are observable and they can be calculated with

$$\hat{\dot{\boldsymbol{x}}}_{des} = A\hat{\boldsymbol{x}}_{des} + \boldsymbol{k}_o(v\kappa_r - C\hat{\boldsymbol{x}}_{des}), \tag{27}$$

where

$$\hat{\boldsymbol{x}}_{des} = \left[\hat{\delta}_{des} \; \hat{\beta}_{des} \; \hat{\dot{\psi}}_{des} \; \hat{\delta}_{cdes}\right]^T$$

is an estimate of $\boldsymbol{x}_{des}$, and

$$A = \begin{bmatrix} a_{11} & 0 & 0 & b \\ a_{21} & a_{22} & a_{23} & 0 \\ a_{31} & a_{32} & a_{33} & 0 \\ 0 & 0 & 0 & 0 \end{bmatrix}, \qquad C = \begin{bmatrix} a_{21} \\ a_{22} \\ 1 + a_{22} \\ 0 \end{bmatrix}^T, \qquad (28)$$

are the system matrix and the measurement matrix, respectively. $\boldsymbol{k}_o$ is an 5×1 observer coefficient matrix, which can be calculated through the pole placement or the LQR-method. The efficiency of the observer will be shown later with simulation results.

In (26), it is implied that the steering command δ_{cdes} is a constant for the observer design. However, with a high observer gain $\boldsymbol{k}_o$, a rapid convergence of $\hat{\delta}_{cdes}$ to δ_{cdes} can be achieved. Nevertheless, the observer gain should be tailored to avoid undesired "nervous" observer outputs in a real vehicle path tracking application, especially, if the curvature of the path captured by a sensor is noisy.

Similar to the feedback control coefficient $\boldsymbol{k}_c$, the observer coefficient $\boldsymbol{k}_o$ can be designed for different vehicle speeds to achieve speed dependent desired observer dynamics.

Finally, substituting the desired states $\delta_{des}, \beta_{des}, \dot{\psi}_{des}$ and the desired steering command δ_{cdes} in (19) and (20) with the estimated values $\hat{\delta}_{des}, \hat{\beta}_{des}, \hat{\dot{\psi}}_{des}, \hat{\delta}_{cdes}$, it results in:

$$\delta_{LQR} = -\boldsymbol{k}_c \boldsymbol{x}_e \,, \qquad (29)$$

$$\delta_c = \delta_{LQR} + \hat{\delta}_{cdes} \,, \qquad (30)$$

where $\boldsymbol{x}_e$ is now defined as

$$\boldsymbol{x}_e = [\hat{\delta}_e \;\; \hat{\beta}_e \;\; \hat{\dot{\psi}}_e \;\; \psi_e \;\; y_L]^T. \qquad (31)$$

Equation (29) and (30) describe the final controller with the state feedback δ_{LQR} and the feedforward steering command $\hat{\delta}_{cdes}$.

5. SIMULATION RESULTS

Simulations have been performed in MATLAB to demonstrate the efficiency of the developed control strategy. The vehicle model parameters used in the simulations are presented in Table 1. The sampling time used is 10 ms and no assumption of a constant longitudinal speed has been made.

Table 1. Vehicle Model Parameters

Parameter	Description	Value
$m[kg]$	Mass	1744.00
$J_z[kg \times m^2]$	Yaw moment of inertia	2825.00
$c_r\ [N/rad]$	Rear cornering stiffness	177800.00
$c_f\ [N/rad]$	Front cornering stiffness	135000.00
$l_r[m]$	Rear axle to CoG distance	1.62
$l_f[m]$	Front axle to CoG distance	1.43
a_{11}	EPS parameter 1	-2.801
b	EPS parameter 2	2.801

The observer coefficient matrix $\boldsymbol{k}_o$ has been designed with the pole placement method. The values of $\boldsymbol{k}_o$ with corresponding speed are shown in Table 2.

Table 2. Observer Gain Matrix

v_x [m/s]	$k_o(1)$	$k_o(2)$	$k_o(3)$	$k_o(4)$
10.0	-31.9973	-22.6158	-180.9843	170.8645
15.0	15.8719	0.3644	-58.1470	168.1563
20.0	30.8573	7.0144	27.0266	139.9722
25.0	37.0846	8.8263	77.3579	128.0911
30.0	41.0621	9.3655	115.3127	123.0737
35.0	44.2948	9.4696	147.6546	121.5400
40.0	47.2454	9.4009	177.0357	122.0016
45.0	50.0827	9.2577	204.6854	123.7069
50.0	52.8755	9.0813	231.2437	126.2376

The speed dependent feedback controller coefficients were calculated with the speed dependent weighting matrices Q and R. The values are given in Table 3.

Table 3. LQR Controller Gain Matrix

v_x[m/s]	$k_c(1)$	$k_c(2)$	$k_c(3)$	$k_c(4)$	$k_c(5)$
10.0	3.445	0.9805	0.2735	4.9338	0.8944
15.0	3.911	1.6567	0.3488	5.5592	0.7303
20.0	4.200	2.3316	0.4018	6.1684	0.6325
25.0	4.394	2.9903	0.4404	6.7596	0.5657
30.0	4.530	3.6295	0.4693	7.3322	0.5164
35.0	4.628	4.2487	0.4913	7.8863	0.4781
40.0	4.700	4.8486	0.5083	8.4226	0.4472
45.0	4.754	5.4301	0.5214	8.9420	0.4216
50.0	4.793	5.9941	0.5317	9.4455	0.4000

The path to be followed (blue) is shown in Figure 4. The curvature of the path and the prescribed vehicle's speed are shown in Figure 3, where the x-axis represents the length s of the path. The initial position and yaw angle of the simulated vehicle are the same as those of the path's starting point.

5.1 Tracking with LQR feedback controller only

First, we demonstrate the efficiency of the full error-state feedback controller. For this purpose, only the states feedback control δ_{LQR} is used to generate the steering command, namely: $\delta_c = \delta_{LQR.}$

In Figure 4 and Figure 5, we see that the lateral deviation y_L is kept under 0.025 m. Furthermore, the maximum yaw angle error is under 0.0286° over the whole simulation distance of 25 km. Even though only the feedback steering control δ_{LQR} has been used, the tracking performance of the proposed

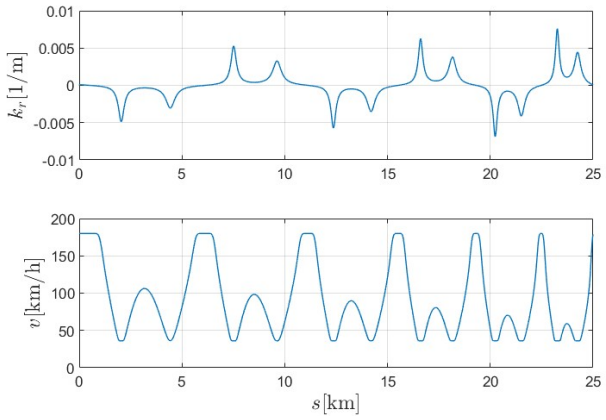

Fig. 3. Curvature κ_r and vehicle speed v over path distance.

control strategy is already excellent. The superior performance of the proposed control strategy can be mainly attributed to the full error states feedback and the excellent accuracy of the reference states obtained by the proposed desired states observer.

In particular, the steering angle error $\hat{\delta}_e$ and the yaw rate error $\dot{\hat{\psi}}_e$ in the full error states feedback act as derivative terms of yaw angle error ψ_e and lateral displacement y_L and enable an earlier response of the controller against the increasing of tracking errors. Additionally, the feedback of the side slip angle $\hat{\beta}_e$ contributes to eliminating small tracking errors caused by non-zero curvature of the path.

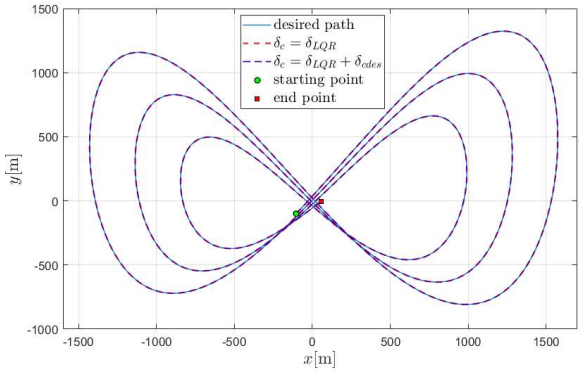

Fig. 4. Simulated vehicle paths with LQR feedback controller only (red) and with both LQR feedback and feedforward controller (violet) versus the desired path (blue).

5.2 *Tracking with both LQR feedback and feedforward controller*

Now we simulate the vehicle tracking control with both the state feedback control δ_{LQR} and the feedforward steering δ_{cdes} as the steering command, namely: $\delta_c = \delta_{LQR} + \hat{\delta}_{cdes}$.

The simulation results are depicted in Figure 4 and Figure 6. The maximum yaw angle error is under 0.0218° and the maximum lateral deviation of the vehicle position is under 0.002 m over the whole simulation distance, which is less than one tenth of those obtained from the LQR feedback controller only.

It can be observed from Figure 6 that the steering command δ_c is almost identical to the desired steering command $\hat{\delta}_{cdes}$. This demonstrates that the proposed control strategy is efficiently integrates the road curvature into the equivalent desired steering command and the corresponding desired state.

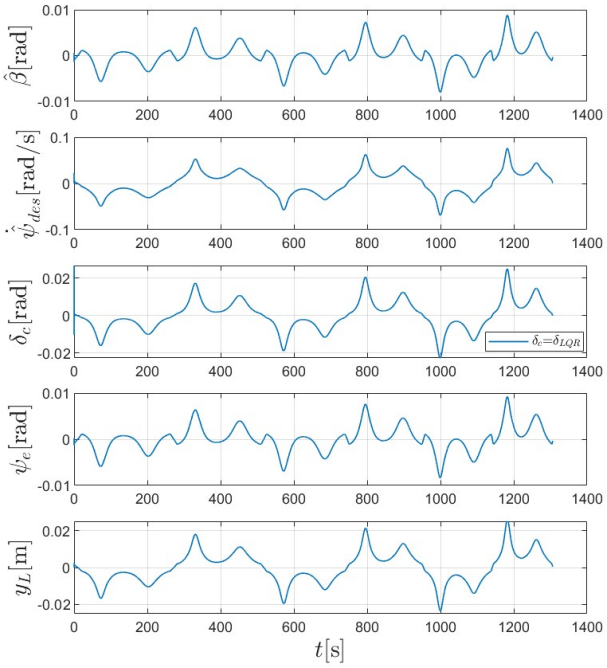

Fig. 5. Vehicle states over time with LQR controller only.

Note that even though the feedback controller δ_{LQR} has very little contribution to the magnitude of the final steering command δ_c in our simulation, it nonetheless guarantees the tracking success through error states feedback control.

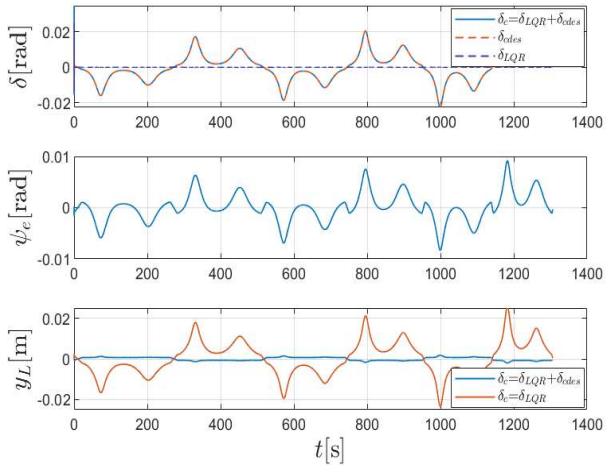

Fig. 6. Closed loop simulation with both $\hat{\delta}_{cdes}$ and δ_{LQR}.

5.3 Robustness of the controller

Finally, to investigate the robustness of the proposed control strategy against the vehicle model uncertainties, the same observer coefficient and LQR controller coefficient shown in Table 1 and Table 2 are deployed in simulations with the following modified vehicle parameters:

- 30% reduced vehicle mass m and inertia J_z
- 30% increased vehicle mass m and inertia J_z
- 30% reduced tire cornering stiffness c_f and c_r
- 30% increased tire cornering stiffness c_f and c_r.

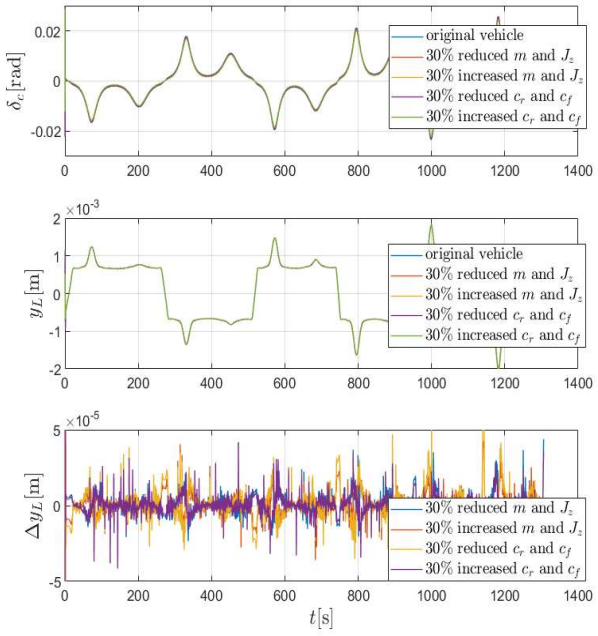

Fig. 7. Simulation with modified vehicle model parameter.

It can be seen from the simulation results shown in Figure 7 that the vehicle parameter uncertainties in the considered scope have very low impact on the tracking control results, even though the observer and the controller parameters are not adapted to the changed vehicle parameters. The tracking controller designed with the proposed control strategy seems robust against vehicle model uncertainties.

6. CONCLUSION

This paper presents a novel control strategy for vehicle path following and trajectory tracking. The newly introduced vehicle lateral full error-state dynamic equation incorporates more significant error states than conventional error-state equations and enables the straightforward design of the full error-state feedback controller without having to consider varying path curvature as an uncontrollable disturbance input unlike previous solutions. The developed desired state observer almost exactly maps the varying curvature of the desired path into a feedforward steering command. It simultaneously delivers the necessary desired reference states to construct the full error-states and thus realizes tracking control.

The presented simulations demonstrate the efficiency, high-performance and robustness of the developed control strategy for vehicle lateral motion control.

Although the control strategy has been developed for vehicle path following control, the strategy can be used for the tracking controller design of many other linear systems. Especially, for tracking problems where the signals to be tracked are not explicitly available as system reference states and reference input, the presented method can be used to reconstruct this lacking information to realize a full error-state feedback and feedforward tracking control.

REFERENCES

Eykhoff, P. (1974) *System Identification – Parameter and State estimation*. London John Wiley & Sons.

Kapania, N.R. and Gerdes, J. C. (2015). Design of a feedback-feedforward steering controller for accurate path tracking and stability at the limits of handling. *Vehicle System Dynamics*, Volume 53, Issue 12, 2015, 1687-1704

Kramer, U. (2008) *Kraftfahrzeug-führung: Modellle – Simulation – Regelung* HANSER

Li, L. and Wang, F. (2005) Research Advances In Vehicle Lateral Motion Monitoring And Control. *International Journal of Intelligent Control and Systems,* volume 10, No. 1, 60-76.

Marino, R., Scalzi, S., Orlando, G. and Netto, M. (2009). A Nested PID Steering Control for Lane Keeping in Vision Based Autonomous Vehicles. *American Control Conference* 2885-2890.

Mitschke, M. and Wallentowitz, H. (2004). *Dynamik der Kraftfahrzeuge*. Springer

Ni, L., Gupta, A., Falcone, P. and Johannesson, L. (2016) Vehicle Lateral Motion Control with Performance and Safety Guarantees, *IFAC-PapersOnLine* 49-11 (2016) 285–290

Rajamani, R. (2012). *Vehicle Dynamics and Control.* 2nd ed. Springer

Schmeitz, A., Zegers, J., Ploeg, and Alirezaei, M (2017). Towards a generic lateral control concept for cooperative automated driving theoretical and experimental evaluation. *5th IEEE International Conference on Models and Technologies for Intelligent Transportation Systems* 134–139

Tagne, G., Talj, R. and Charara, A. (2016). Design and Comparison of Robust Nonlinear Controllers for the Lateral Dynamics of Intelligent Vehicles. *IEEE Transactions on Intelligent Transportation Systems*, VOL. 17, NO. 3, MARCH 2016 796-809

Yin, X. (2010). Verfahren und Systeme zur Fahrspurenmittenführung eines Kraftfahrzeugs. https://register.dpma.de/DPMAregister/pat/PatSchriftteneinsicht?docId=DE102010033530A1